Original Research Article

ARE THE PHYSICAL PARAMETERS WITH THE SUPPORT VECTOR MACHINE (SVM) METHOD ABLE TO CLASSIFY BENIGN AND MALIGNANT?

ARTICLE INFO

Keywords:

Mammography

Benign

Malignant

SVM

Physical Parameters

ABSTRACT

Objective: Evaluating the diagnostic performance of SVM to classify benign and malignant by performing a meta-analysis.

Method: The data used for this study were secondary data. It consisted of 221 mammogram images (mean age 57.5 years) with 164 malignant and 57 benign, taken from a radiological database that has been examined by a radiologist with more than 20 years of experience. Also, histopathological record data has been examined by an oncologist with more than 20 years of experience. Mammograms were taken from January 2022 to June 2022. In addition, 221 mammograms consisting of 164 malignant and 57 benign were used as SVM method training, and 20 mammograms consisting of 10 malignant and 10 benign were used to test the performance of the SVM method. Then, it was evaluated using pathology results as the gold standard.

Result: Benign had a significantly lower Deviation (an average of 29.2661230 ± 10.14916673) than malignant (an average of 33.1841234 ± 11.70238757). The SVM method performance value obtained the values of TP, FP, TN, FN, accuracy, sensitivity, Specificity, and Precision, respectively 7,7, 3, 3, 50%, 70%, 30%, and 50%.

Conclusion: A proper performance to distinguish benign and malignant can be obtained using the physical deviation parameters with the SVM classification approach. However, these findings should be

proven in larger datasets and several with different mammographic scanners. Our meta-analysis shows that the physical parameters and SVM have high sensitivity but low specificity. Of the nine physical parameters in the mammogram, only the parameter deviation was significant to distinguish between benign and malignant. The SVM method proved to be able to differentiate between benign and malignant.

1. Introduction

A biopsy is a relatively expensive invasive method, and there is an increasing demand for non-invasive diagnostic methods that reduce the number of biopsies [1]. Mammography has become a diagnostic standard that is inexpensive, non-invasive, and easy to apply. It is used to diagnose breast cancer, especially in areas that are not too dense. Physical parameters and SVM methods now play an essential role in differentiating the lesions detected by mammography to improve diagnostic assessment. Each mammogram has a different pixel intensity value depending on the breast density value. Physical parameter values have different patterns depending on the distance between pixels. Benign and malignant pixel intensity values have different patterns. Therefore, this study aimed to evaluate the diagnostic performance of SVM to classify benign and malignant by conducting a meta-analysis.

2. Materials and Methods

2.1. Mammogram

Firstly, patient records were taken from a radiology room whose histopathological value was confirmed and had been examined by an oncologist with more than 20 years of experience. After getting the patient record data, take mammogram images from the radiology room database according to the patient record data. Not all patient data records had mammogram images because not all patients performed mammography examinations at the hospital. Mammogram data was secondary data taken from the Dokter Soetomo Surabaya hospital database from January 2022 to June 2022. Mammograms that met the following inclusion criteria were included in this study. 1) A mammogram with a suspicious breast lesion was detected, and the record data was in the oncology room. 2) The patient did not undergo biopsy, chemotherapy, or other interventions before the examination. 3) The diameter of the breast lesion was greater than 1cm. 4) Pathology confirmed the characteristics of the lesion. Of the two hundred and thirty data, only two hundred and twenty-one met the inclusion criteria.

2.2. Image Acquisition

The mammogram images were taken from a Kodak of mammography brand machine, dryview 6800 laser imager with settings KV= 30, MAS = 25, brightness =

7, latitude = 11, contrast = -4, film size = 18x24 cm.

2.3. Image Analysis

A radiologist had more than 20 years of experience diagnosing breast lesions and analyzing mammogram images. ROI was selected in the area of the most apparent lesion with a size of 2 x 2 cm. Then, a contrast correction mammogram was performed. The physical parameters on the mammogram were calculated automatically using the formula [2]. Further, the results of these calculations were tabulated using Excel, and the entropy values of benign and malignant were collected into one file, as well as the other eight physical parameters. Then, it continued to conduct the statistical analysis. The study also made visual separation of the background with suspicious mass objects. Furthermore, it will be seen whether there is a visual difference between benign (fibroadenoma, Epithelial, Lipoma, Cystic) and malignant (Invasive Ductal Carcinoma, Invasive Lobular Carcinoma).

2.4. Statistical Analysis

The data of nine physical parameters with a normal distribution were expressed as mean ± SD. In addition, it was compared using the T-test to determine the difference in the values of the physical parameters at certain distances between pixels to classify benign and malignant. The Anova test was used to determine whether the values of the same physical parameters at different distances between pixels had different values. Besides, the Manova test was used to determine whether the values of different physical parameters at the same distance had statistically different means and whether the values of all parameters at the same distance had statistically different mean values.

3. Results

Table 1 reports that postoperative pathological examination confirmed a total of 221 lesions, mean age of 57.5 years (57 benign and 164 malignant).

Figure 1 reports the visualization of object separation against the background of each type of benign and malignant.

Table 2 reports the mean, standard deviation, homogeneity, and p.value of the T-test results to select significant physical parameters to differentiate benign and malignant.

Figure 2 reports a box plot of benign and malignant against physical parameters to show the higher physical parameters values between benign and malignant.

Table 3 reports the mean, standard deviation, homogeneity, and p.value on the difference in the values of the physical parameters at distances I and j.

Table 4 reports the mean, standard deviation, homogeneity, and p.value of each physical parameter for all distances from 1 pixel to 10 pixels.

Table 5 reports the mean, standard deviation, homogeneity, and p.value of all physical parameters to the distance between pixels singly.

Figure 3 reports the data before and after being separated by SVM.

3.1. Pathological Findings

Table 1. Histopathological types of 221 confirmed breast lesions

Binign (N=57)		Malignant (N=164)	
Fibroadenoma Epithelial	31 4	Invasive Ductal	156

Lipoma Cystic	4 18	Carcinoma Invasive Lobular	 8

		Carcinoma	

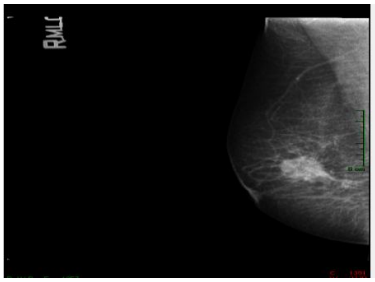

(a)

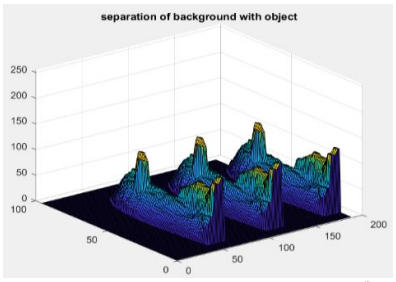

(b)

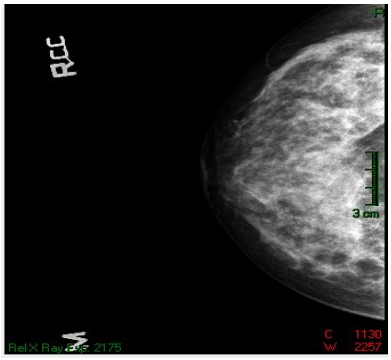

(c)

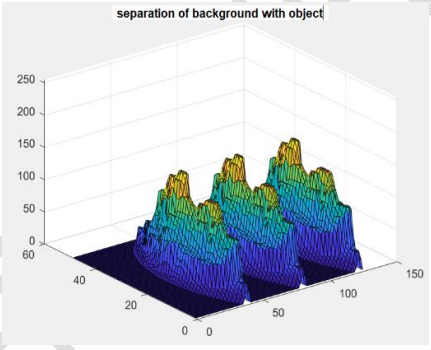

(d)

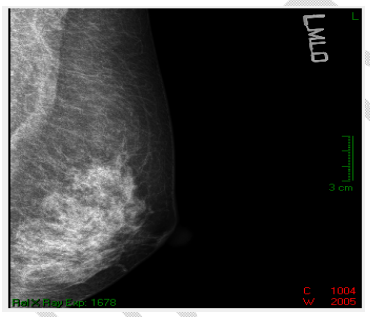

(e)

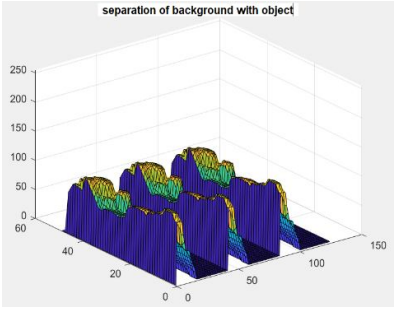

(f)

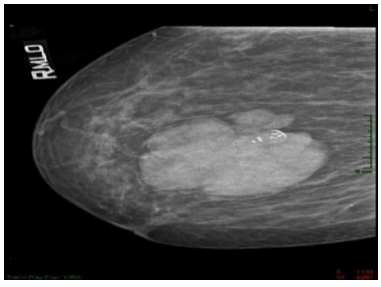

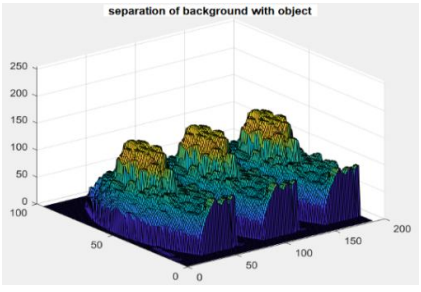

(g) (h)

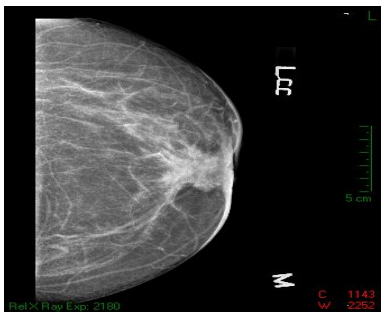

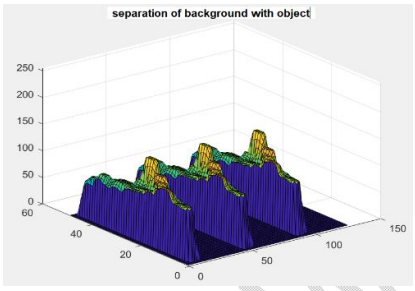

(i) (j)

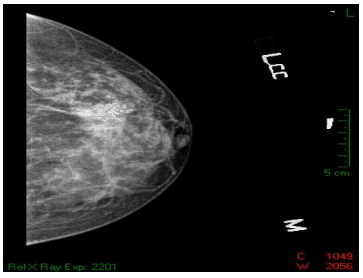

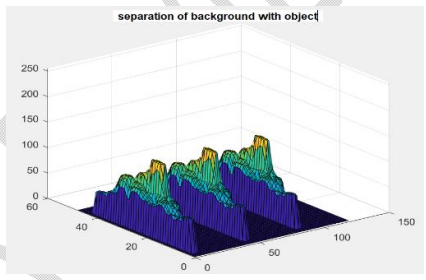

(k) (l)

Fig 1 (a) original fibroadenoma, (b) visual separation of background with fibroadenoma object, (c) original epithelial, (d) visual separation of background with an epithelial object, (e) original lipoma, (f) visual separation of background with lipoma object, (g) original cystic, (h) visual separation of the background from the cystic object, (i) original Invasive Lobular Carcinoma, (j) visual separation of the background from the object Invasive Lobular Carcinoma, (k) original Invasive Ductal Carcinoma, (l) visual separation of the background with object Invasive Ductal Carcinoma

Table 2. The T-test results determine the type of physical parameters that can distinguish benign and malignant.

Physical parameters	d	Types of cancer	N	Mean ± SD	Homogeneity of Variances	P.Value
Deviation	1	benign	57	29.2661230 ± 10.14916673	0.081	0.025
		malignant	164	33.1841234 ± 11.70238757		
	2	benign	57	28.5529330 ± 9.35366579	0.028	0.005
		malignant	164	32.9303829 ± 11.52254507		
	3	benign	57	28.9365904 ± 9.91777120	0.088	0.031
		malignant	164	32.6469437 ± 11.51886027		
	4	benign	57	28.8757035 ± 9.88459275	0.085	0.025
		malignant	164	32.7302653 ± 11.53222758		
	5	benign	57	28.7876132 ± 9.90266631	0.094	0.025
		malignant	164	32.6556002 ± 11.53067204		

6	benign malignant	57 164	28.7310381 ± 9.90323495 32.5526713 ± 11.51487323	0.108	0.026
7	benign malignant	57 164	28.6428042 ± 9.90462508 32.9683803 ± 12.45179698	0.073	0.018
8	benign malignant	57 164	28.6340682 ± 9.92132520 32.4748835 ± 11.54323733	0.105	0.026
9	benign malignant	57 164	28.6236523 ± 9.94634886 32.4376877 ± 11.53288829	0.126	0.027
10	benign malignant	57 164	28.6039161 ± 9.96439906 32.4558556 ± 11.52533616	0.134	0.026

d = distance between pixels, N = number of data, SD = standard deviation

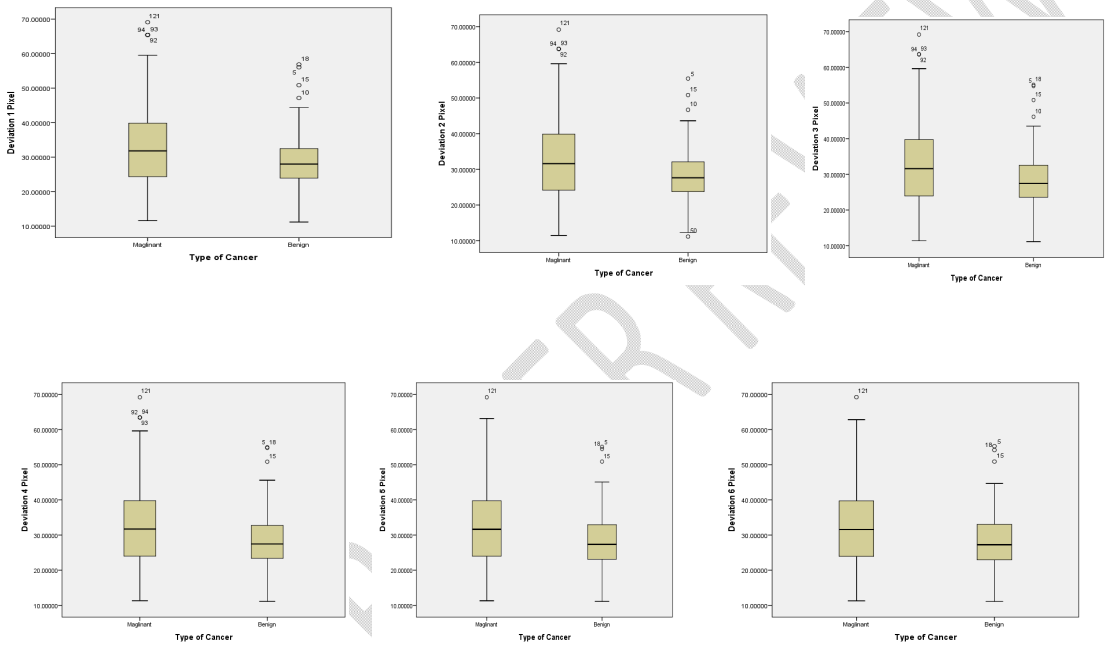

The explore deviation results can be described in Figure 2.

Fig 2 box plot of deviation values at a distance of 1, 2, 3, 4, 5, and 6 pixels from benign and malignant (57 benign, 164 malignant). The plot shows benign deviation values are lower than malignant ($p < 0.05$).

Table 3 Anova test results to find out whether there is a difference in the value of physical parameters at a distance from I to j

Types	N	parameter	Distance between pixels I to j		mean±SD	Homogeneity of Variances	P.value Anova	P.value Multiple Comparisons
			Distance between pixels i	Distance between pixels j				
Benign	57	EntrHd	1	2	1.5221330 ± 0.10771850	0.236	0.000	0.005

				3	1.5221330 ± 0.10771850	0.236	0.000	0.000
				4	1.5221330 ± 0.10771850	0.236	0.000	0.000
				5	1.5221330 ± 0.10771850	0.236	0.000	0.000
				6	1.5221330 ± 0.10771850	0.236	0.000	0.000
				7	1.5221330 ± 0.10771850	0.236	0.000	0.000
				8	1.5221330 ± 0.10771850	0.236	0.000	0.000
				9	1.5221330 ± 0.10771850	0.236	0.000	0.000
				10	1.5221330 ± 0.10771850	0.236	0.000	0.000
Benign	57	MD	1	2	0.0550107 ± 0.01569023	0.752	0.000	0.002
				3	0.0550107 ± 0.01569023	0.752	0.000	0.000
				4	0.0550107 ± 0.01569023	0.752	0.000	0.000
				5	0.0550107 ± 0.01569023	0.752	0.000	0.000
				6	0.0550107 ± 0.01569023	0.752	0.000	0.000
				7	0.0550107 ± 0.01569023	0.752	0.000	0.000
				8	0.0550107 ± 0.01569023	0.752	0.000	0.000
				9	0.0550107 ± 0.01569023	0.752	0.000	0.000
				10	0.0550107 ± 0.01569023	0.752	0.000	0.000
Malignant	164	Entropy	1	2	3.6001343 ± 0.15934733	0.991	0.000	0.153
				3	3.6001343 ± 0.15934733	0.991	0.000	0.003
				4	3.6001343 ± 0.15934733	0.991	0.000	0.000
				5	3.6001343 ± 0.15934733	0.991	0.000	0.000
				6	3.6001343 ± 0.15934733	0.991	0.000	0.000
				7	3.6001343 ± 0.15934733	0.991	0.000	0.000
				8	3.6001343 ± 0.15934733	0.991	0.000	0.000
				9	3.6001343 ± 0.15934733	0.991	0.000	0.000
				10	3.6001343 ± 0.15934733	0.991	0.000	0.000

Table 4. The Manova test results to determine the physical parameters for all distances that have an effect on classifying benign and malignant.

Physical parameters	d	Types	N	Mean±SD	Homogeneity of Variances	P.Value
Entropy	1	Maglinant	164	3.6001343 ± 0.15934733	0.000	0.005
		Benign	57	3.5773911 ± 0.16166549		
	2	Maglinant	164	3.6480609 ± 0.16057995	0.000	0.005
		Benign	57	3.6239189 ± 0.16332596		
	3	Maglinant	164	3.6693990 ± 0.16088320	0.000	0.005
		Benign	57	3.6464661 ± 0.16407282		
	4	Maglinant	164	3.6804048 ± 0.16025254	0.000	0.005
		Benign	57	3.6572530 ± 0.16306310		
	5	Maglinant	164	3.6872418 ± 0.15872824	0.000	0.005
		Benign	57	3.6627882 ± 0.16174247		
	6	Maglinant	164	3.6883574 ± 0.15968949	0.000	0.005
		Benign	57	3.6645679 ± 0.16010536		
	7	Maglinant	164	3.6915338 ± 0.15625152	0.000	0.005

		Benign	57	3.6644747 ± 0.15802681		
	8	Maglinant	164	3.6899345 ± 0.15480639	0.000	0.005
		Benign	57	3.6640172 ± 0.15749139		
	9	Maglinant	164	3.6879138 ± 0.15298895	0.000	0.005
		Benign	57	3.6597479 ± 0.15357946		
	10	Maglinant	164	3.6849469 ± 0.15126207	0.000	0.005
		Benign	57	3.6557046 ± 0.15088854		
MeanHd	1	Maglinant	164	13.2438160 ± 3.43451516	0.000	0.006
		Benign	57	12.8762181 ± 3.10649959		
	2	Maglinant	164	16.7932382 ± 4.83522335	0.000	0.006
		Benign	57	16.1712349 ± 4.31987597		
	3	Maglinant	164	19.2259412 ± 5.61510019	0.000	0.006
		Benign	57	18.6196667 ± 5.37123718		
	4	Maglinant	164	21.2548643 ± 6.34683180	0.000	0.006
		Benign	57	20.4479156 ± 6.08728499		
	5	Maglinant	164	22.9757829 ± 6.99544098	0.000	0.006
		Benign	57	21.9850772 ± 6.73826805		
	6	Maglinant	164	24.5326754 ± 7.60246639	0.000	0.006
		Benign	57	23.3428314 ± 7.34602432		
	7	Maglinant	164	25.8645163 ± 8.09585975	0.000	0.006
		Benign	57	24.4792261 ± 7.81579842		
	8	Maglinant	164	27.0155987 ± 8.51634185	0.000	0.006
		Benign	57	25.4672005 ± 8.18642617		
	9	Maglinant	164	28.1721550 ± 9.06922846	0.000	0.006
		Benign	57	26.1694923 ± 8.55513045		
	10	Maglinant	164	29.2466852 ± 9.60529810	0.000	0.006
		Benign	57	27.0714639 ± 8.73614556		

Table 5. The Manova test results for all physical parameters to the distance between pixels singly

Physical parameters	d	Types	N	mean±SD	Homogenity	p.value
Entropy	10	Maglinant	164	3.6849469±0.15126207	0.000	0.013
		Benign	57	3.6557046±0.15088854		
Contras	10	Maglinant	164	1644.7461898±1142.08121172	0.000	0.013
		Benign	57	1381.8808921±901.92299339		
MA	10	Maglinant	164	0.0006111±0.00343260	0.000	0.013
		Benign	57	0.0003630±0.00296724		
MD	10	Maglinant	164	0.0271359±0.00911123	0.000	0.013
		Benign	57	0.0288426±0.01030822		
mean	10	Maglinant	164	139.4617544±29.80848920	0.000	0.013
		Benign	57	136.0219377±33.14379894		
dev	10	Maglinant	164	32.4558556±11.52533616	0.000	0.013
		Benign	57	28.6039161±9.96439906		
EntrHd	10	Maglinant	164	1.8578421±0.14898065	0.000	0.013
		Benign	57	1.8316384±0.14303157		

MAngHd	10	Maglinant	164	0.0180974±0.00712905	0.000	0.013
		Benign	57	0.1349186±0.43074903		
MeanHd	10	Maglinant	164	29.2466852±9.60529810	0.000	0.013
		Benign	57	27.0714639±8.73614556		

Discussions

Background separation visualization with the object is seen differently for each histopathology type, such as benign (fibroadenoma, Epithelial, Lipoma, Cystic) and malignant (Invasive Ductal Carcinoma, Invasive Lobular Carcinoma) (Figure 1).

Deviation physics parameter values are arduous to separate between benign and malignant, as shown in Figure 3 (a). After using the SVM method, the deviation physics parameter values are separated between benign and malignant, as shown in Figure 3(b).

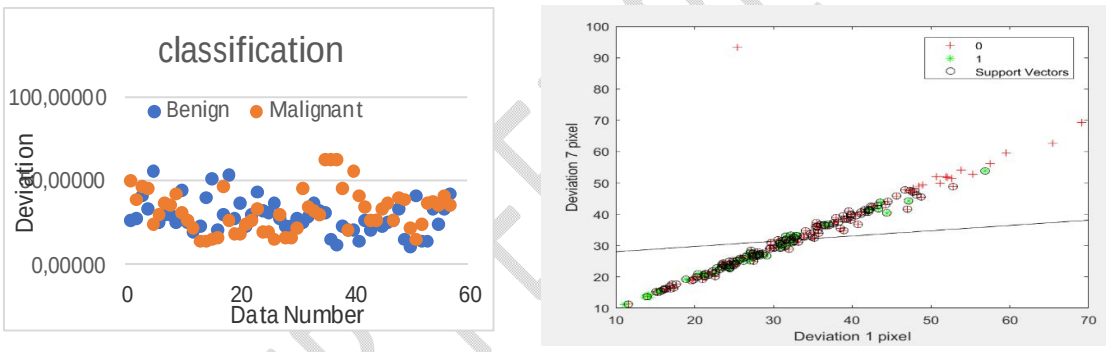

(a) (b)

Fig 3 (a) Data before using SVM, (b) data after using SVM

Table 6 SVM test results using the deviation parameter

Dev1	Dev7	Prediction	Actual	TP	FP	TN	FN
27.98022	27.48027	1	1	1	0	0	0
56.05074	55.47237	0	1	0	0	0	1
30.31202	30.08855	1	1	1	0	0	0
27.61248	25.70893	1	1	1	0	0	0
24.67097	22.76627	1	1	1	0	0	0
50.86057	50.99776	0	1	0	0	0	1
29.65246	30.02081	1	1	1	0	0	0
35.48983	36.26204	0	1	0	0	0	1
12.32340	12.10034	1	1	1	0	0	0
23.92487	24.65912	1	1	1	0	0	0

36.69807	38.30339	0	0	0	0	1	0
45.83331	45.78140	0	0	0	0	1	0
31.51387	29.87651	1	0	0	1	0	0
37.54308	35.05740	0	0	0	0	1	0
30.37775	30.89288	1	0	0	1	0	0
21.75716	21.51413	1	0	0	1	0	0
13.89439	13.47330	1	0	0	1	0	0
17.73907	16.61927	1	0	0	1	0	0
19.77592	19.03029	1	0	0	1	0	0
23.85646	23.77035	1	0	0	1	0	0
			Total	7	7	3	3

Dev1 parameter deviation at a distance of 1 pixel, Dev7 parameter deviation at a distance of 7 pixels, TP True Positive, FP false Positive, TN True Negative, FN False Negative.

Table 7 Results of benign and malignant classification using threshold

D1	D2	D1- D2	Prediction	Actual	TP	FP	TN	FN
0.05012	0.04256	0.00756	1	1	1	0	0	0
0.03708	0.03004	0.00704	1	1	1	0	0	0
0.06146	0.04680	0.01466	1	1	1	0	0	0
0.05379	0.04264	0.01115	1	1	1	0	0	0
0.05330	0.04847	0.00483	0	1	0	0	0	1
0.03943	0.03411	0.00532	0	1	0	0	0	1
0.04473	0.03646	0.00827	1	1	1	0	0	0
0.04161	0.03280	0.00881	1	1	1	0	0	0
0.08645	0.07345	0.01300	1	1	1	0	0	0
0.11333	0.09338	0.01995	1	1	1	0	0	0
0.05682	0.04301	0.01381	1	0	0	1	0	0
0.04380	0.03507	0.00873	1	0	0	1	0	0
0.07326	0.05492	0.01834	1	0	0	1	0	0
0.05309	0.03865	0.01444	1	0	0	1	0	0
0.04287	0.03648	0.00639	1	0	0	1	0	0
0.07036	0.05946	0.01090	1	0	0	1	0	0
0.05621	0.05202	0.00419	0	0	0	0	1	0
0.05893	0.05480	0.00413	0	0	0	0	1	0
0.07013	0.06758	0.00255	0	0	0	0	1	0
0.03135	0.02845	0.00290	0	0	0	0	1	0
				Total	8	6	4	2

D1 value of Inverse Differential Moment at a distance of 1 pixel, and D2 value of Inverse Differential Moment at a distance of 2 pixels.

From the T-test results, it found that Benign's physical parameters had a significantly lower Deviation (mean 29.2661230 ± 10.14916673) than malignant (mean 33.1841234 ± 11.70238757) with homogeneity value > 0.05 and p.value < 0.05 (Table 2).

From the ANOVA test, the physical parameters of Inverse Differential Moment (MD) and entropy of Hdiff (EntrHd) have homogeneity values > 0.05 and p.value < 0.01. It means that the physical parameters of Inverse Differential Moment (MD) and entropy of Hdiff (EntrHd) can be used as threshold methods to classify benign and

malignant (table 3). The threshold value we used is 0.006 if it is greater than the threshold predicted to be benign. The classification results obtained the values of TP, FP, TN, FN, accuracy, sensitivity, Specificity, and Precision, respectively 8, 6, 4, 2, 60%, 80%, 40%, and 57% (Table 7).

From the Manova test, each physical parameter to all the distances between pixels, the entropy, and meanHd parameters has heterogeneous data (homogeneity < 0.05) and p.value < 0.01 (table 4).

From the Manova test of all physical parameters for each distance between pixels, a distance of 10 pixels has heterogeneous data (homogeneity < 0.05) and p.value < 0.02 (table 5).

Research on the classification of benign and malignant breast cancer is active research. Many have been reported to distinguish between benign and malignant. For instance, Khamis et al. reported that benign sonoelastrographic strain ratio values were lower than malignant [1]. Awad reported that malignant areas were stiffer than their surroundings, appeared darker, had higher contrast, was larger in diameter, more tightly bound to the surrounding tissue, and had greater elasticity than benign [3]. Abd El-A;eem et al. reported that the Apparent Diffusion Coefficient (ADC) of malignant was lower than benign [4]. Mus et al. reported that the To investigate time to enhancement (TTE) malignant value was less than 12.96 seconds than benign [5]. Li et al. reported that benign had a longer time to peak (TTP) than malignant, and the strengthening intensity (SI) of malignant was higher than benign [6]. Forte et al. reported that the ratios of the scattering and absorption signal (R-value) of malignant were smaller than benign [7]. W.Ma et al. reported that Malignant had greater restriction of water molecule movement than benign [8]. Demirler Simsir et al. reported that the iodine content of malignant was much higher than benign [9]. D. Ma et al. reported that malignant cells grew more rapidly and were irregular in shape than benign [10]. Kanao et al. reported that the Apparent Diffusion Coefficient (ADC) of high T2 signal intensity (SI) in malignant was greater than in benign [11]. Fusco et al. reported that malignant had more blood vessels and deoxyhemoglobin than benign [12]. Zhang et al. reported that the speed of benign Quantitative Transport Mapping (QTM) was lower than that of malignant [13]. While Fuller et al. reported that vascular density was significantly reduced in high-grade tumors [14]. Han et al. reported that malignant orientation-aware cfDNA fragmentation (OCF) values were higher than benign [15]. Papachristopoulou et al. reported that the value of Human kallikrein-related peptidase 12 (KLK12) malignant was greater than benign [16]. Wubulihasimu et al. reported that benign had a regular edge shape while malignant was irregular [17]. Chen et al. reported that the perfusion fraction (f) and Distributed Diffusion Coefficient (DDC) values of malignant were lower than benign [18].

CONCLUSION

A proper performance to distinguish benign and malignant can be obtained using the physical deviation parameters with the SVM classification approach. However, these findings should be proven in larger datasets and several with different mammographic scanners. Our meta-

analysis shows that the physical parameters and SVM have high sensitivity but low specificity. Of the nine physical parameters in the mammogram, only the parameter deviation was significant to distinguish between benign and malignant. The SVM method proved to be able to differentiate between benign and malignant.

BIBLIOGRAPHY

[1] M. E. M. Khamis, A. M. Alaa El-deen, and A. A. Azim Ismail, "The diagnostic value of sonoelastographic strain ratio in discriminating malignant from benign solid breast masses," *Egyptian Journal of Radiology and Nuclear Medicine*, vol. 48, no. 4, pp. 1149–1157, Dec. 2017, doi: 10.1016/j.ejrnm.2017.05.005.

[2] A. A. N. Gunawan, S. Poniman, and I. W. Supardi, "Classification of breast cancer grades using physical parameters and K-nearest neighbor method," *Telkomnika (Telecommunication Computing Electronics and Control)*, vol. 17, no. 2, pp. 637–644, Apr. 2019, doi: 10.12928/TELKOMNIKA.V17I2.9797.

[3] F. M. Awad, "Role of supersonic shear wave imaging quantitative elastography (SSI) in differentiating benign and malignant solid breast masses," *Egyptian Journal of Radiology and Nuclear Medicine*, vol. 44, no. 3, pp. 681–685, Sep. 2013, doi: 10.1016/j.ejrnm.2013.04.001.

[4] R. A. Abd El-Aleem, E. Abo El-Hamd, H. A. Yousef, M. E. M. Radwan, and R. A. A. Mohammed, "The added value of qualitative and quantitative diffusion-weighted magnetic resonance imaging (DW-MRI) in differentiating benign from malignant breast lesions," *Egyptian Journal of Radiology and Nuclear Medicine*, vol. 49, no. 1, pp. 272–280, Mar. 2018, doi: 10.1016/j.ejrnm.2017.10.015.

[5] R. D. Mus *et al.*, "Time to enhancement derived from ultrafast breast MRI as a novel parameter to discriminate benign from malignant breast lesions," *European Journal of Radiology*, vol. 89, pp. 90–96, Apr. 2017, doi: 10.1016/j.ejrad.2017.01.020.

[6] J. Li *et al.*, "Can different regions of interest influence the diagnosis of benign and malignant breast lesions using quantitative parameters of contrast-enhanced sonography?," *European Journal of Radiology*, vol. 108, pp. 1–6, Nov. 2018, doi: 10.1016/j.ejrad.2018.09.005.

[7] S. Forte *et al.*, "Can grating interferometry-based mammography discriminate benign from malignant microcalcifications in fresh biopsy samples?," *European Journal of Radiology*, vol. 129, Aug. 2020, doi: 10.1016/j.ejrad.2020.109077.

[8] W. Ma, J. Mao, T. Wang, Y. Huang, and Z. H. Zhao, "Distinguishing between benign and malignant breast lesions using diffusion weighted imaging and intravoxel incoherent motion: A systematic review and meta-analysis," *European Journal of Radiology*, vol. 141, Aug. 2021, doi: 10.1016/j.ejrad.2021.109809.

[9] B. Demirler Şimşir, K. B. Krug, C. Burke, M. Hellmich, D. Maintz, and E. Coche, "Possibility to discriminate benign from malignant breast lesions detected on dual-layer spectral CT-evaluation," *European Journal of Radiology*, vol. 142, Sep. 2021, doi: 10.1016/j.ejrad.2021.109832.

[10] D. Ma *et al.*, "Intravoxel incoherent motion diffusion-weighted imaging as an adjunct to dynamic contrast-enhanced MRI to improve accuracy of the differential diagnosis of benign and malignant breast lesions," *Magnetic Resonance Imaging*, vol. 36, pp. 175–179, Feb. 2017, doi: 10.1016/j.mri.2016.10.005.

[11] S. Kanao, M. Kataoka, M. Iima, D. M. Ikeda, M. Toi, and K. Togashi, "Differentiating benign and malignant inflammatory breast lesions: Value of T2 weighted and diffusion weighted MR images," *Magnetic Resonance Imaging*, vol. 50, pp. 38–44, Jul. 2018, doi: 10.1016/j.mri.2018.03.012.

[12] R. Fusco *et al.*, "Blood oxygenation level dependent magnetic resonance imaging and diffusion weighted MRI imaging for benign and malignant breast cancer discrimination," *Magnetic Resonance Imaging*, vol. 75, pp. 51–59, Jan. 2021, doi: 10.1016/j.mri.2020.10.008.

[13] Q. Zhang *et al.*, "Quantitative transport mapping (QTM) for differentiating benign and malignant breast lesion: Comparison with traditional kinetics modeling and semi-quantitative enhancement curve characteristics.," *Magnetic Resonance Imaging*, vol. 86, pp. 86–93, Feb. 2022, doi: 10.1016/j.mri.2021.10.039.

[14] A. M. Fuller *et al.*, "Vascular density of histologically benign breast tissue from women with breast cancer: associations with tissue composition and tumor characteristics," *Human Pathology*, vol. 91, pp. 43–51, Sep. 2019, doi: 10.1016/j.humpath.2019.06.003.

[15] B. W. Han *et al.*, "Noninvasive discrimination of benign and malignant breast lesions using genome-wide nucleosome profiles of plasma cell-free DNA," *Clinica Chimica Acta*, vol. 520, pp. 95–100, Sep. 2021, doi: 10.1016/j.cca.2021.06.008.

[16] G. Papachristopoulou *et al.*, "Human kallikrein-related peptidase 12 (KLK12) splice variants discriminate benign from cancerous breast tumors," *Clinical Biochemistry*, vol. 58, pp. 78–85, Aug. 2018, doi: 10.1016/j.clinbiochem.2018.05.017.

[17] M. Wubulihasimu, M. Maimaitusun, X. L. Xu, X. D. Liu, and B. M. Luo, "The added value of contrast-enhanced ultrasound to conventional ultrasound in differentiating benign and malignant solid breast lesions: a systematic review and meta-analysis," *Clinical Radiology*, vol. 73, no. 11, pp. 936–943, Nov. 2018, doi: 10.1016/j.crad.2018.06.004.

[18] B. Y. Chen *et al.*, "Multiple b-value diffusion-weighted imaging in differentiating benign from malignant breast lesions: comparison of conventional mono-, bi- and stretched exponential models," *Clinical Radiology*, vol. 75, no. 8, pp. 642.e1-642.e8, Aug. 2020, doi: 10.1016/j.crad.2020.03.039.